PERFORMANCE ANALYSIS OF TAYLOR-SERIES LINEARIZATION SCHEME OF 1ST ORDER ON THE DISCRETIZATION OF MOVEMENT EQUATIONS WITH VORONOI DIAGRAMS

Alonso, Ewerton Eyre de Morais
Universidade do Vale do Itajai, 5ª Avenida s/n, Bairro dos Municípios, Balneário Camboriú, Santa Catarina, CEP 88330-000.
ewerton.eyre@univali.br

Peters, Sérgio
Universidade Federal de Santa Catarina, Campus Universitário, Trindade, Cx. Postal 476, Florianópolis, SC, CEP 8804-900.
peters@inf.ufsc.br

Abstract. *This paper presents the description, analysis, implementation and comparison of an alternative linearization on discretization of Navier-Stokes' equations using Taylor-series linearization of 1st order, analogous to the Newton's Method applied to the resolution of non linear Equations, using UpWind Difference Scheme (UDS) of 1st order on the Finite Volume Method with non-structured meshes generated by Voronoi Diagrams. The Conjugated Gradient method was used to solve the linear equation system resulted from the discretization of Navier-Stokes' equation, with velocities u and v evaluated throughout the UDS interpolation. The laminar incompressible flow on a squared cavity of finite depth with a sliding superior wall with steady velocity, like a treadmill, was used to validate the numeric results. The obtained results allowed conclude that the linearization using Taylor-series linearization presented best performance, in some test cases, than the Separation linearization.*

Keywords*: Taylor-series Linearization, Finite Volumes, Voronoi Diagrams, Navier-Stokes' Equations.*

1. Introduction

On Computational Fluid Dynamics (CFD), most of the applications involve numeric methods with fluid flow on complex geometries (Ronzani and Nieckele, 1995) in which are appropriate the use of adapted meshes to the problem's geometry. Among such meshes, the non-structured meshes generated by the Voronoi Diagram (VD), which are independent of any global coordinate, stand out (Taniguchi *et al.*, 1991a) (Marcondes, 1996). One of the applications of VDs is the generation of non-structured meshes to numeric discretization of partial differential equations (EDPs).

The numeric discretization of Navier-Stokes' EDPs could be done throughout Finite Volume Method (FVM) (Patankar, 1980), which consists on the physical domain division in non overlapped finite number of control volume (CV), where local balance from involved physical variables are promoted.

This paper presents the description, analysis, implementation and comparison to an alternative linearization on discretization of Navier-Stokes' equations using Taylor-series linearization of 1st order, analogous to the Newton's Method applied to the resolution to non linear equations, using UDS interpolation of 1st order, on the FVM with non-structured meshes generated by VD. Moreover, this paper has the purpose to compare the Separation linearization performance (with UDS) (Mariani, 1997) (Cardoso, 1997) with the alternative linearization proposed.

2. Navier-Stokes Equation Discretization throughout Finite Volume Method

The discretization process of Navier-Stokes' equation throughout FVM (Cardoso, 1997) generates:

$$Ap_i^0(\varphi_i-\varphi_i^0)+\sum_{j=1}^{NV(i)}\left[\rho W\varphi-\Gamma^{\varphi}\frac{\partial\varphi}{\partial z}\right]_{ij}S_{ij}=S_i^{\varphi}\Delta\vartheta_i \tag{1}$$

Where:

Ap_i^0 → Nodal point *i* Coefficient.
ρ_i → Specific fluid mass in the nodal point *i*.
t → Time.
$\Delta\vartheta_i$ → CV Volume from a polygonal convex prism generated trough VD.
φ_i^0 → Generic φ variable evaluated in the previous time (*t*).
φ_i → Generic φ variable evaluated in the time $t+\Delta t$.
i → Generic Control Volume (CV).
j → Neighbor index for *i*.
NV → Number of neighbors for *i*.
W_{ij} → Normal velocity Component evaluated on *ij* face.
Γ^{φ} → Diffusion coefficient for φ.

L_{ij} → Distance between *i* and *j*.

S_{ij} → Face (edge) between two generic points *i* and *j*.

S_i^{φ} → Is the source term for φ on the CV *i*.

$\left.\frac{\partial\varphi}{\partial z}\right|_{ij} = \frac{\varphi_i - \varphi_j}{L_{ij}}$ → Approach for Central Difference of 1st order ($E_T = O^2$).

The advective-difusive flux of φ (where z is the normal direction to *ij* face) is given by (Cardoso, 1997):

$$J_{ij} = \left[\rho W\varphi - \Gamma^{\varphi}\frac{\partial\varphi}{\partial z}\right]_{ij} \tag{2}$$

On Equation (2) the index variables *ij* are evaluated over the *ij* interface throughout the adequate average to each case (Patankar, 1980), i.e., $\rho_{ij} = \frac{\rho_i + \rho_j}{2}$, $\Gamma_{ij}^{\varphi} = \frac{2\Gamma_i\Gamma_j}{\Gamma_i + \Gamma_j}$ and $\left.\frac{\partial\varphi}{\partial z}\right|_{ij} = \frac{\varphi_i - \varphi_j}{L_{ij}}$.

W_{ij} could be evaluated through Eq. (3) (ex_{ij} and ey_{ij} are *x* and y components from normal unit vector to the CV's). This approximation has been used and generates stabled numerical approximations (Patankar, 1980) (Maliska, 1995).

$$W_{ij} = u_{ij}\, ex_{ij} + v_{ij}\, ey_{ij} \tag{3}$$

After the discretization using FVM, a non-linear equation system of 2nd order is acquired, and needs some kind of linearization to be solved iteratively like a linear system equation.

3. Linearization using Taylor-series formulation of 1st order

The advective-difusive flux for a generic variable φ through a face is calculated using the Eq. (2). When $\varphi = u$ or $\varphi = v$ there is nonlinearity involved on term $\rho W\varphi$, and $\rho W\varphi$ must be linearized to allow that the algebraic system must be solved like a linear system equation. Traditionally, W_{ij} is obtained from previous iterations velocity values (denoted with *) and φ is evaluated in the new iteration generating the Separation linearization.

Thus, this work has the objective to evaluate $\rho W\varphi$ using Taylor-series linearization of 1st Order (Alonso, 1999). This kind of linearization was chosen because produces quadratically convergent approximations (Faires and Burden, 1993), although the convergence rates to boundaries aren't maintained.

3.1. Navier-Stokes' Equations Discretization

Writing $\varphi_{ij} = u_{ij}$ in the advective term represented in the 1st term on Eq. (2) the obtained term is:

$$G(u_{ij}, v_{ij}) = \rho_{ij} W_{ij} u_{ij} \tag{4}$$

Substituting the Eq. (3) in the Eq. (4) and linearized it using Taylor-series expansion of 1st order:

$$G(u_{ij}, v_{ij}) \cong G(u_{ij}^*, v_{ij}^*) + \left.\frac{\partial G}{\partial u_{ij}}\right|_{u_{ij}^*, v_{ij}^*}(u_{ij} - u_{ij}^*) + \left.\frac{\partial G}{\partial v_{ij}}\right|_{u_{ij}^*, v_{ij}^*}(v_{ij} - v_{ij}^*) \tag{5}$$

$$\left.\frac{\partial G}{\partial u_{ij}}\right|_{u_{ij}^*, v_{ij}^*} = \rho_{ij}(u_{ij}^* ex_{ij} + v_{ij}^* ey_{ij}) + \rho_{ij} ex_{ij} u_{ij}^* = \rho_{ij} W_{ij}^* + \rho_{ij} ex_{ij} u_{ij}^* \tag{6}$$

$$\left.\frac{\partial G}{\partial v_{ij}}\right| = \rho_{ij} ey_{ij} u_{ij}^* \tag{7}$$

$$G(u_{ij}, v_{ij}) = \rho_{ij} W_{ij}^* u_{ij}^* + \left(\rho_{ij} W_{ij}^* + \rho_{ij} ex_{ij} u_{ij}^*\right)\left(u_{ij} - u_{ij}^*\right) + \left(\rho_{ij} ey_{ij} u_{ij}^*\right)\left(v_{ij} - v_{ij}^*\right) \tag{8}$$

The complete equation to the advective-difusive flux, Eq. (2), when $\varphi_{ij} = u_{ij}$ where the diffusive term is evaluated by central difference, can be written by the followed equation:

$$J_{ij} = \rho_{ij} \left\{ u_{ij}^* \left[ex_{ij} \left(2u_{ij} - u_{ij}^* \right) + ey_{ij} \left(v_{ij} - v_{ij}^* \right) \right] + v_{ij}^* ey_{ij} u_{ij} \right\} - \mu_{ij} \left(\frac{u_j - u_i}{L_{ij}} \right) \tag{9}$$

Using the segregated solution for equations system, u_i is solved separately from v_i and v variation is not considerate using $v_{ij} = v_{ij}^*$ on Eq. (9).

Writing $\varphi_{ij} = v_{ij}$ in the advective term represented in the 1st term on Eq. (2) the obtained term is:

$$H\left(u_{ij}, v_{ij}\right) = \rho_{ij} W_{ij} v_{ij} \tag{10}$$

Then, substituting Eq. (3) on Eq. (10) similar to $G\left(u_{ij}, v_{ij}\right)$, $H\left(u_{ij}, v_{ij}\right)$ is linearized using Taylor-series expansion of 1st order. Then, the complete equation to the advective-difusive flux, Eq. (2), to $\varphi_{ij} = v_{ij}$, where the diffusive term is evaluated by Central Difference, can be written by the followed equation:

$$J_{ij} = \rho_{ij} \left\{ v_{ij}^* \left[ey_{ij} \left(2v_{ij} - v_{ij}^* \right) + ex_{ij} \left(u_{ij} - u_{ij}^* \right) \right] + u_{ij}^* ex_{ij} v_{ij} \right\} - \mu_{ij} \left(\frac{v_j - v_i}{L_{ij}} \right) \tag{11}$$

Finally, the segregated solution for equations system is used solving v_i separately from u_i and u variation is not considerated using $u_{ij} = u_{ij}^*$ on Eq. (17).

3.2. Generic Interpolation to u_{ik} and v_{ik}, between the Nodal Points *i* and its neighbors *r*(*k*)

The *W* velocity on a generic *ik* interface, according to Fig. 1, is evaluated by Eq. (3).

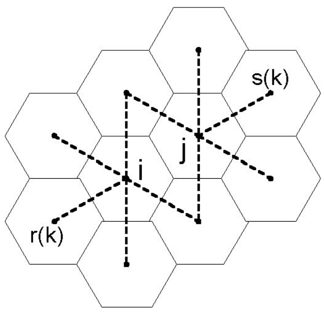

Figure 1. Nodal neighbors *i* and *j* and their respective neighborhood *r*(*k*) and *s*(*k*).

To evaluate *u* and *v* on *ik* interface the UDS scheme can be used, generating the follow linear interpolation for u_{ik} :

$$u_{ik} = u_i \, \delta_{ik}^+ + u_{r(k)} \, \delta_{ik}^- \tag{12}$$

Where $\delta_{ik}^+ = max \frac{(0, F_{ik})}{|F_{ik}|} = \Psi(F_{ik})$ and $\delta_{ik}^- = max \frac{(0, - F_{ik})}{|F_{ik}|} = \Psi(- F_{ik})$ and the mass flux F_{ik} across each *ik* interface is:

$$\Psi(F_{ik}) = \begin{cases} 1, if \ F_{ik} > 0 \\ 0, if \ F_{ik} \leq 0 \end{cases} \tag{13}$$

Alternatively, u_{ik} can be evaluated using CDS as:

$$u_{ik} = \frac{\left(u_i + u_{r(k)}\right)}{2} \tag{14}$$

If $W_{ik}^{*} > 0$ then $\delta_{ik}^{+} = 1$ and $\delta_{ik}^{-} = 0$, so $u_{ik} = u_i$. By the other way, if $W_{ik}^{*} < 0$ then $\delta_{ik}^{+} = 0$ and $\delta_{ik}^{-} = 1$, so $u_{ik} = u_{r(k)}$.
The generic interpolation to v_{ik} can be obtained by the analogous way that was demonstrated to u_{ik} :

$$v_{ik} = v_i\, \delta_{ik}^{+} + v_{r(k)}\, \delta_{ik}^{-} \tag{15}$$

3.3. Discretized Movement Equations with UDS Interpolation for u_{ik} and v_{ik}

Substituting the advective-difusive equation flux for $\varphi_{ik} = u_{ik}$, Eq. (9) on Eq. (1) and on the resulted equation substitute the Eq. (12) and the Eq. (15) the followed equation was generated:

$$Ap_i^u\, u_i + \sum_{k=1}^{NV(i)} \beta_{ik}^u\, \delta_{ik}^{-}\, v_i = \sum_{k=1}^{NV(i)} \left(A_{ik}^u\, u_{r(k)} - \beta_{ik}^u\, \delta_{ik}^{-}\, v_{r(k)} \right) + \Omega_{ik}^u(i) + Ap_i^0\, u_i^0 \tag{16}$$

$$A_{ik}^u = -\left(\alpha_{ik}^u + F_{ik} \right) \delta_{ik}^{-} + D_{ik}^u \text{ and } \alpha_{ik}^u = \rho_{ik} u_{ik}^{*} ex_{ik} S_{ik}$$
$$Ap_i^u = A_{ik}^u\, u_{r(k)} - \beta_{ik}^u\, \delta_{ik}^{-}\, v_{r(k)} \text{ and } \beta_{ik}^u = \rho_{ik} u_{ik}^{*} ey_{ik} S_{ik}$$
$$\Omega_{ik}^u(i) = S_i^u\, \Delta\vartheta_i + \sum_{k=1}^{NV(i)} \left(\alpha_{ik}^u u_{ik}^{*} + \beta_{ik}^u v_i^{*} \right)$$

To not consider the variations effects of v_i on u_i equations, $\beta_{ik}^u = 0$ was used directly on Eq. (16). Then:

$$Ap_i^u\, u_i = \sum_{k=1}^{NV(i)} A_{ik}^u\, u_{r(k)} + b_i^u \tag{17}$$

$$b_i^u = \Omega_{ik}^u(i) + Ap_i^0 u_i^0 \text{ with } \Omega_{ik}^u(i) = S_i^u\, \Delta\vartheta_i + \sum_{k=1}^{NV(i)} \left(\alpha_{ik}^u u_{ik}^{*} \right)$$
$$Ap_i^u = Ap_i^0 + \sum_{k=1}^{NV(i)} \left(\alpha_{ik}^u + F_{ik} \right) \delta_{ik}^{-} + D_{ik}^u \text{ with } D_{ik}^u = \mu_{ik} \left(\frac{S_{ik}}{L_{ik}} \right) \text{ and } F_{ik} = \rho_{ik} W_{ik}^{*} S_{ik}$$

Where u_i^0 is the velocity in *i* point on the previous time and u_{ik}^{*}, v_{ik}^{*} and W_{ik}^{*} are evaluated on the *ik* interface based on a simple arithmetic average between *i* and *r*(*k*).

For the mass conservation equation an integral process is done on CV. Using the Divergence Theorem the integral volume is reduced to an integral face. The discrete sums of all fluxes F_{ik} in each face S_{ik} from CV must be null:

$$\sum_{k=1}^{NV(i)} F_{ik} = 0 \tag{18}$$

$$F_{ik} = \alpha_{ik}^u + \varepsilon_{ik}^u \tag{19}$$

Where $\alpha_{ik}^u = \rho_{ik} u_{ik}^{*} ex_{ik} S_{ik}$ and $\varepsilon_{ik}^u = \rho_{ik} v_{ik}^{*} ey_{ik} S_{ik}$.

To the u_i equation:

$$u_i = \delta_{ik}^{+} u_i + \delta_{ik}^{-} u_i \tag{20}$$

Rewriting Eq. (18) and multiplying it for the u_i equation, given by Eq. (20), the next equation is obtained:

$$\sum_{k=1}^{NV(i)} \left(\alpha_{ik}^u + \varepsilon_{ik}^u \right) \left(\delta_{ik}^{+} u_i + \delta_{ik}^{-} u_i \right) = 0 \tag{21}$$

Subtracting the Eq. (21) from Eq. (16):

$$Ap_i^u \; u_i = \sum_{k=1}^{NV(i)} A_{ik}^u \; u_{r(k)} + b_i^u \tag{22}$$

$$Ap_i^u = Ap_i^0 + \sum_{k=1}^{NV(i)} A_{ik}^u - \alpha_i^u$$

Remember that to $\varphi = u$, the source term S_i^u has the pressure term (Cardoso, 1997). Then:

$$Ap_i^u \; u_i = \sum_{k=1}^{NV(i)} A_{ik}^u \; u_{r(k)} + b_i^u - \Delta\vartheta_i (\nabla P)_i^x \tag{23}$$

$$Ap_j^u \; u_j = \sum_{k=1}^{NV(i)} A_{jk}^u \; u_{s(k)} + b_j^u - \Delta\vartheta_j (\nabla P)_j^x \tag{24}$$

The discretized movement equations with UDS to v_{ik} could be obtained in an analog way that was showed to u_{ik} .

3.4. Pressure Equation

Until the present moment, just evolutive equation for *u* and another for *v* were obtained, governed by an advective-difusive equation. The pressure is just a variable of general equations, without a specific evolutive equation. To solve this problem the SIMPLE-method is used between the velocity and pressure, modified for colocated meshes (Peric *et al.*, 1988) and Cardoso (1997). Thus, the *u* and *v* equations on *i* and *j* nodal points - Eq. (23), Eq. (24) - and their analogous equations for *v* on normal direction $\hat{e}_{ij}$ produce:

$$(w_i)_{ij} = \frac{1}{Ap_i^u}\left(\sum_{k=1}^{NV(i)} A_{ik}^u \; u_{r(k)} + b_i^u - \Delta\vartheta_i (\nabla P)_i^x\right) ex_{ij} + \frac{1}{Ap_i^v}\left(\sum_{k=1}^{NV(i)} A_{ik}^v \; v_{r(k)} + b_i^v - \Delta\vartheta_i (\nabla P)_i^y\right) ey_{ij} \tag{25}$$

$$(w_j)_{ij} = \frac{1}{Ap_j^u}\left(\sum_{k=1}^{NV(j)} A_{jk}^u \; u_{s(k)} + b_j^u - \Delta\vartheta_j (\nabla P)_j^x\right) ex_{ij} + \frac{1}{Ap_j^v}\left(\sum_{k=1}^{NV(j)} A_{jk}^v \; v_{s(k)} + b_j^v - \Delta\vartheta_j (\nabla P)_j^y\right) ey_{ij} \tag{26}$$

$(w_i)_{ij}$ and $(w_j)_{ij}$ are evaluated on the *ij* normal direction, respectively, over *i* and *j* nodal points. Thus, the velocity component over *ij* interface is given by:

$$W_{ij} = \frac{(w_i)_{ij} + (w_j)_{ij}}{2} \tag{27}$$

Substituting Eq. (25) and Eq. (26) in Eq. (27), an equation to W_{ij} can be defined by Eq. (28), considering an arithmetic average for the independent pressure terms and $d_{ij}^w (\nabla P)_{ij}^w$ approaches the pressure dependent gradient terms:

$$W_{ij} = \hat{W}_{ij} - d_{ij}^w \, (\nabla P)_{ij}^w \tag{28}$$

$$\hat{W}_{ij} = 0.5\left[\frac{1}{Ap_i^u}\left(\sum_{k=1}^{NV(i)} A_{ik}^u \; u_{r(k)} + b_i^u\right) ex_{ij} + \frac{1}{Ap_i^v}\left(\sum_{k=1}^{NV(i)} A_{ik}^v \; v_{r(k)} + b_i^v\right) ey_{ij}\right] + \\ + 0.5\left[\frac{1}{Ap_j^u}\left(\sum_{k=1}^{NV(j)} A_{jk}^u \; u_{s(k)} + b_j^u\right) ex_{ij} + \frac{1}{Ap_j^v}\left(\sum_{k=1}^{NV(j)} A_{jk}^v \; v_{s(k)} + b_j^v\right) ey_{ij}\right] \tag{29}$$

$$d_{ij}^w = 0.25\left[\Delta\vartheta_i\left(\frac{1}{Ap_i^u} + \frac{1}{Ap_i^v}\right) + \Delta\vartheta_j\left(\frac{1}{Ap_j^u} + \frac{1}{Ap_j^v}\right)\right] \tag{30}$$

$$(\nabla P)_{ij}^w = \frac{(P_j - P_i)}{L_{ij}} \tag{31}$$

Eqs. (29) and (30) are generated through an approached sequence defined by Eq. (27). On this way the pressure gradient used in Eq. (31) considers the W_{ij}'s neighbors pressures, respectively the values after and before W_{ij}, which are a physically consistent formulation, according to Peric *et al.* (1988).

W_{ij} can be either evaluated like UDS interpolation proposed to u_{ij} and v_{ij}, according to Eq. (32), but the evaluation made by Eq. (27) gave more stable numerical results, under the test cases.

$$W_{ij} = \delta_{ij}^{+} w_i + \delta_{ij}^{-} w_j \tag{32}$$

4. Results and Conclusions

The test used to evaluate the linearization with their respective interpolations proposed in this work was the laminar incompressible flow on a squared finite depth cavity with a sliding superior wall (lid-driven cavity square) with steady velocity, like a treadmill. Inferior and lateral walls are impermeable. The boundary conditions used were:

- Right lateral wall: x = L, $y = 0$, $u = v = 0$.
- Left lateral wall: $x = 0$, $u = v = 0$.
- Inferior wall: $y = 0$, $u = v = 0$.
- Superior wall: y = L, $u = 1$, $v = 0$.
- Width of the mesh: $L = 32.10$ (value chosen in function of the mesh).

A computational program was used to solve the proposed problem (Cardoso, 1997), in which there were implemented the linearization and their respective interpolations compared in this work, simulating the stationary fluid flow, although the implemented program permits the temporal discretization too. The solution to the linear equations system generated from discretization was obtained through Conjugated Gradient method (Mariani, 1997) (Golub, 1989) and the pressure gradient used was the proposed by Taniguchi *et al.* (1991a) and Taniguchi and Kobayashi (1991b). The computer used was an IBM 9076 SP/2 because the program and the method used were previously developed in IBM AIX operating system. However, the program developed in this work uses serial programming.

For u and v velocities it was adopted the 0.7 relaxation. For the pressure it was used 0.5. The internal repetition number for u and v velocities was two, while for pressure was three. It was adopted $u = v = 0.5$ for initials velocity conditions and for pressure $P = 0$. The results were collected with Reynolds numbers 100 and 1000 calculated by:

$$Re = \rho \frac{U.L}{\mu} \tag{33}$$

Where U is the superior wall movement speed ($U = 1$), L is the cavity width ($L = 32.10$), ρ is the specific fluid mass ($\rho = 1$) and μ is the dynamic fluid viscosity (it varies as the desired Reynolds number).

As convergence criteria (according to the desired precision, $\xi = 1.\ 10^{-5}$) it was used:

$$error_i^k = \sum_{j=1}^{NV(i)} \left| F_{ij}^k \right| < \xi \tag{34}$$

To evaluated u and v, Eq. (12) and Eq.(15) were used. In test cases it was used a mesh of hexagonal volumes with 6400 nodal points generated through VD (mesh generated to the generator of VD of Maliska Jr. (1994)). To the boundary, the program allowed to use a unique neighbor to all nodal points connected to a wall; which was useful for the proposal system solution. It's important to point out that the boundary conditions could be inserted in the discretized equations, but this wasn't made because more than a condition of boundary in each side of the mesh wasn't needed.

4.1. Results Analysis

The obtained results with Taylor-series linearization were compared with the results obtained with Separation linearization (with UDS) (Mariani, 1997) and (Cardoso, 1997), under the same conditions as described on the previous section and with the results obtained by Ghia *et. al.* (1982). The figures shown on the next subsections present the graphics with the u and v velocity profiles for Reynolds 100 and 1000 throughout a central vertical line ($x = L / 2$) and horizontal central line ($y = L / 2$) for the velocities in directions x and y, respectively, on the used mesh.

4.1.2. Results Obtained with Reynolds 100

The Figure 2 presents the graphics for velocity u profile throughout a central vertical line and the velocity v profile throughout a central horizontal line, respectively. To the graphics showed in Fig. 2 the results obtained with both linearization (Separation and Taylor-series) were very close when compared to each other and sometimes overlapped to the results obtained by Ghia *et. al.* (1982), but when compared with Ghia *et. al.* (1982), they are closer for *u* than *v*.

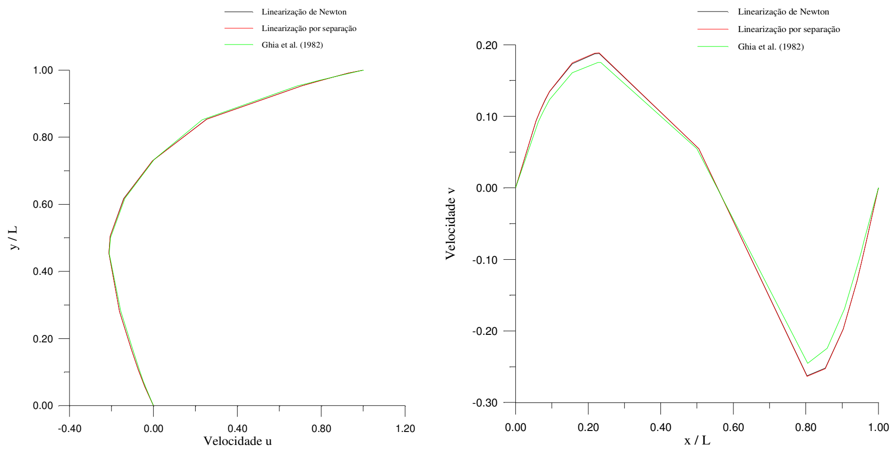

Figure 2. *u* and v velocity profile graphics throughout a central line - *R*e = 100.

It was possible to conclude that Taylor-series linearization presented best performance than Separation linearization when considerate the number of iterations and CPU time needed for the convergence of the system equation - Tab. 1.

Table 1. Taylor-series Linearization versus Separation Linearization - *Re* = 100.

Linearization type	Number of Iterations	CPU time (minutes)	Velocity[35].*u*
Separation	1654	24,05	-0.004896
Taylor-series	1309	18,28	-0.004895

4.1.3. Results Obtained with Reynolds 1000

The Figure 3 presents the graphics of the velocity *u* profile throughout a central vertical line and the velocity *v* profile throughout a central horizontal line, respectively. By analyzing the graphics showed in Fig. 3 the results obtained with both linearization (Separation and Taylor-series) were very close when compared each other and sometimes overlapped to the results obtained by Ghia *et. al.* (1982). The obtained results presented in Fig. 3 show a *u* and *v* velocity profile relatively far from the obtained results by Ghia *et. al.* (1982).

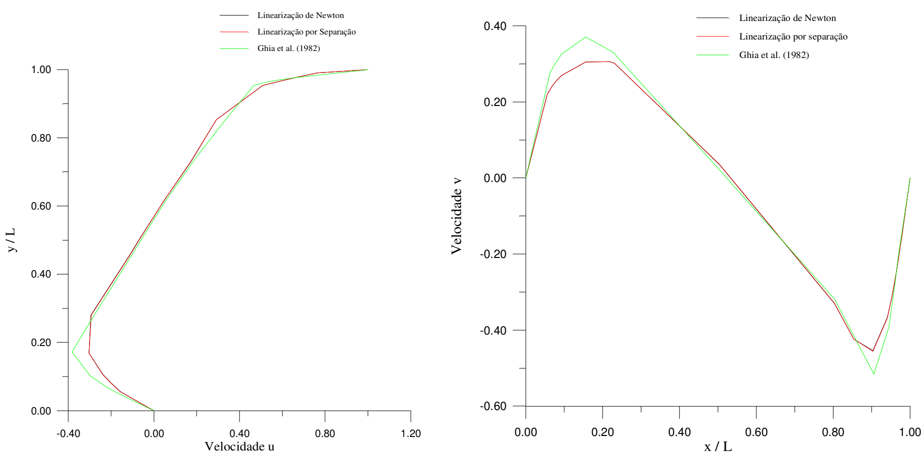

Figure 3. *u* and v velocity profile graphics throughout a central line - *Re* = 1000.

Table 2. Taylor-series Linearization versus Separation Linearization - *Re* = 1000.

Linearization type	Number of Iterations	CPU time (minutes)	Velocity[35].*u*
Separation	2325	32,17	-0.021100
Taylor-series	2516	37,27	-0.020983

It was possible to conclude that Taylor-series linearization presented worse performance than Separation linearization considerating the number of iterations and CPU time needed for the convergence of the system equation - Tab. 2. The value of *u* velocity on the point with number 35 of the used mesh was close in both linearization analyzed.

5. Final Considerations

The main purpose of this work was to optimize the computational cost involved on the solution of the linear system equations generated from discretization. Thus, based on the obtained results, it was possible to conclude that the Taylor-series linearization presented better performance than Separation linearization in some test cases.

During the test cases it was observed that the system equations convergence velocity through Taylor-series linearization was dependent on the way that W_{ij} was evaluated - Eq. (27) and Eq. (32). The system equations convergence using Eq. (32) wasn't obtained. Thus, Eq. (27) was used on all tests. Although it had been presented results for Reynolds's number 100 and 1000 only, tests had been made to Reynolds 10000, but the process of convergence wasn't obtained. Additional tests must be done, in both cases, to obtain more information about this event.

To the velocities *u* and *v* profiles presented on the previous sections, it is important to point out that the mesh used by Ghia *et. al.* (1982) has about 16641 nodal points, while the mesh used on this work has 6400 nodal points disposed in hexagonal volumes.

Finally, it must be emphasized that the present work used segregated solution to equations system because the Conjugate Gradient method with the way it was implemented resolves the *u* and *v* velocities separately.

6. References

Alonso, E. E. de M., 1999, "Análise de Desempenho do Esquema de Linearização de Newton na Discretização das Equações do Movimento com Diagramas de Voronoi", Dissertação de Mestrado, Curso de Pós-graduação em Ciência da Computação do Departamento de Informática e Estatística da Universidade Federal de Santa Catarina, Florianópolis, Brasil.

Cardoso, F. C., 1997, "Algoritmo para Simulação Numérica de Equações do Movimento pelo Método dos Volumes Finitos usando Diagramas de Voronoi", Dissertação de Mestrado, Curso de Pós-graduação em Ciência da Computação do Departamento de Informática e Estatística da Universidade Federal de Santa Catarina, Florianópolis, Brasil.

Faires, J. D., Burden, R. L, 1993, "Numerical Methods", PWS Publishing Company, Boston, USA, 429p.

Ghia, U., Ghia, K. N. and Shin, C. T., 1982, "High-Re Solutions for Incompressible Flow Using the Navier_Stokes Equations and Multigrid Method", Journal of Computacional Physics, Vol.48, pp. 387-411.

Golub, G. H. and O'Leary, D. P., 1989, "Some History of the Conjugate Gradient and Lanczos Algorithms : 1948-1976", SIAM Review, Vol.31, No. 1, pp. 50-102.

Marcondes, F., 1996, "Solução Numérica Usando Métodos Adaptativos-Implícitos e Malhas de Voronoi de Problemas de Reservatório de Petróleo", Tese de Doutorado, Departamento de Engenharia Mecânica da Universidade Federal de Santa Catarina, Florianópolis, Brasil.

Maliska, C. R., 1995, "Transferência de Calor e Mecânica dos Fluidos Computacional", Ed. Livros Técnicos e Científicos S. A., Rio de Janeiro, Brasil, 472 p.

Maliska JR. C. R., 1994, "Um Robusto Gerador de Diagramas de Voronoi para Discretização de Domínios Irregulares", XIV Congresso Ibero Latino-Americano sobre Métodos Computacionais para a Engenharia, Belo Horizonte, Brasil, pp. 548-547.

Mariani, V. C., 1997, "Resolução de Sistemas Lineares Gerados na Discretização das Equações de Navier-Stokes em Malhas de Voronoi", Dissertação de Mestrado, Curso de Pós-graduação em Ciência da Computação do Departamento de Informática e Estatística da Universidade Federal de Santa Catarina, Florianópolis, Brasil.

Patankar, S. V., 1980, "Numerical Heat Transfer and Fluid Flow", Ed. Hemisphere Publishing Corporation, United States of America,197 p.

Peric, M., Kesseler, R. and Scheuerer, G., 1988, "Comparison of Finite Volume Numerical Methods With Staggered and Colocated Grids", Computers & Fluids, Vol.16, pp. 389-403.

Taniguchi, N., Arakawa, C. and Kobayashi, T., 1991, "Construction of a Flow-Simulating Method With Finite Volume Based on a Voronoi Diagram", JSME International Journal, Série III, Vol.34, pp. 18-23.

Taniguchi, N. and Kobayashi, T., 1991, "Finite Volume Method on the Unstructured Grid System", Computers & Fluids, Vol.19, No. 34, pp. 287-295.

Ronzani, E. R. e Nieckele, A. O., 1995, "Método de Solução Numérica de Escoamentos Incompressíveis em Geometrias Complexas", Congresso Ibero Latino Americano sobre Métodos Computacionais para Engenharia, Curitiba, Brasil, pp. 41-50.

7. Responsibility notice

The authors Ewerton Eyre de Morais Alonso and Sérgio Peters are the only responsible for the printed material in this paper.